Desalination and Water Treatment
www.deswater.com

doi: 10.5004/dwt.2018.21811

103 (2018) 141–151
January

Nickel ion removal from aqueous solution using recyclable zeolitic imidazolate framework-8 (ZIF-8) nano adsorbent: a kinetic and equilibrium study

Zohreh Roostan[a], Alimorad Rashidi[b,*], Seyed Mehdi Borghei[c]

[a]*Department of Environmental Engineering, Science and Research Branch, Islamic Azad University, Tehran, Iran, email: zohrehrostan@yahoo.com*
[b]*Nanotechnology Research Center, Research Institute of Petroleum Industry (RIPI), West Blvd. Azadi Sports Complex, P.O. Box 14665-1998, Tehran, Iran, Tel. +982148252092, email: Rashidiam@ripi.ir*
[c]*Department of Chemical and Petroleum Engineering, Sharif University of Technology, Tehran, Iran, email: Mborghei@sharif.edu*

Received 28 June 2017; Accepted 14 December 2017

ABSTRACT

The adsorption of nickel ions in an aqueous solution system was measured using zeolitic imidazolate framework-8 (ZIF-8) nanoadsorbent. ZIF-8 crystals were synthesized using the hydrothermal method. Nanoadsorbent was characterized by FTIR, XRD, SEM and N_2 adsorption analysis. ZIF-8 crystals showed a high surface area of 1303 m^2/g and particle size 100–150 nm. The Langmuir and Freundlich isotherms model were used to analyze the data. The sufficiently high R^2 value of 0.996 resulted from the Langmuir isotherm model demonstrated the perfect performance of this model. The kinetic data were analyzed using the pseudo-first-order and pseudo-second-order models of types 1–4. Kinetic studies of the adsorption showed that the adsorption process followed the pseudo-second-order kinetics model of type 2. Experimental data showed that the maximal adsorption capacity of nickel by ZIF-8 adsorbent was 69.36 mg/g at initial metal ions concentration 25 mg/L at T = 25°C and pH 7.0. Desorption of nickel from spent ZIF-8 was carried out using 0.1 M EDTA solution effectively and recycled at least four times. No reduction in adsorption efficiency was observed up to 3 cycles of adsorption–desorption. The results confirmed the applicability of ZIF-8 as an effective nanoadsorbent for the removal of nickel ions from aqueous solutions.

Keywords: Adsorption; Isotherm; Kinetic; Zeolitic imidazolate framework-8 (ZIF-8); Nickel removal, Aqueous solution

1. Introduction

Recently, the removal of toxic heavy metal ions from wastewater has been widely studied because of their dangerous effects on all organisms including human [1–4]. Nickel is usually presented in the effluents of silver refineries, industrial wastewater from mining, electroplating, zinc base casting and storage battery industries. The maximum permissible concentration of nickel in drinking water should be limited to 0.02 mg/L according to US-EPA report. In humans, nickel can directly lead to emerging serious problems in human including, but not limited to, dermatitis, allergic sensitization, lungs, kidneys, skin and nervous system damages. It is also known as carcinogen [5,6]. As a result of toxic effects of nickel to human and animal life, it is important to treat industrial effluents polluted with nickel ions before their discharge into the receiving water bodies [7]. Conventional methods for the removal of nickel from wastewaters are including chemical precipitation, ion exchange, filtration, chemical reduction, electro-deposition and adsorption [8–10]. However, it is necessary to use an economical, effective, and reliable technique for nickel removal due to operational demerits, complexity and high cost of the treatment. Due to its comparatively low

*Corresponding author.

cost, wide range of applications, simplicity of design, easy operation, low harmful secondary products and facile regeneration of the adsorbents, adsorption has been considered as the best decontamination technique [5,11]. There have been numerous types of sorbents for nickel removal; however, the adsorption capacity of conventional sorbents is generally limited by their chemical properties and irregular pore structures [12].

Metal–organic frameworks (MOFs) are hybrid materials formed during the crystallization of transition metal clusters and functionalized organic ligands coordinating to form one, two and three dimensional porous rigid structures. MOFs have been considered to be novel adsorbents for a variety of applications, because of their high surface areas, large pore volumes, tunable pore geometries, and versatile chemical compositions. In a similar vein, zeolitic imidazolate frameworks are a sub-family of MOFs which consist of M-Im-M (where M stands for Zn, Co cation and Im stands for the imidazolate linker) formed by a self-assembly approach [13]. If imidazole linkers tetrahedrally coordinated with the metallic secondary building units, bond angles can be formed that mimic those of the silicon and oxygen ions in the formation of zeolites. Therefore, it is possible to synthesize ZIFs in the same topological conformations of aluminosilicate zeolites [14]. In addition to typical properties of MOFs including high porosity, tailorable cavity sizes and good affinity with organic polymers, ZIFs are of some special characteristics such as exceptional thermal stability and outstanding chemical resistance [13,15]. Among various ZIFs materials, ZIF-8 crystals will be studied more in depth. There are two main components in a typical ZIF-8 synthesis: a zinc source and the bridging ligand 2-methylimidazole (Hmim). ZIF-8 has SOD topology and pore aperture of 0.34 nm [16]. ZIF-8 exhibits superior thermal stability (up to 400°C) and remarkable resistance to water and to boiling in organic solvents such as benzene and methanol [14,17]. Previously, ZIF-8 has been widely investigated in gas separation, hydrogen storage, carbon dioxide capture, organic size selective separation and catalysis [18–21]. ZIF-8 crystals could be an attractive sorbent for nickel ions removal because of its ultrahigh porosity, high chemical stability and hydrophobic nature. In the current study, the feasibility of adsorptive removal of nickel ions by ZIF-8 crystals is systematically investigated.

The main objective of the current research is to investigate the feasibility of using ZIF-8 crystals for the removal of nickel ions from aqueous solution by varying parameters of agitation time, nickel ions concentration, pH and ZIF-8 concentration. Although the adsorptive removal of nickel ions by using different adsorbents modified holly sawdust [22], activated carbon prepared from coirpith [23], Peganum harmala-L [24], almond husk [25], natural zeolite [26] and Sawdust Xanthate modified with ethanediamine [27] has been reported, there is not an experimental investigation about the application of robust and highly porous ZIFs structures for removal of nickel ions in the literature. Herein, for the first time, we report the adsorption of nickel ions from water on ZIF-8 material. ZIF-8 crystals were synthesized in aqueous solution by consuming excess 2-methyimidazole (2-Hmim). The prepared ZIF-8 crystals were characterized by analyzing scanning electron microscopy coupled with energy-dispersive X-ray spectroscopy (SEM-EDX), powder X-ray diffraction (PXRD), accelerated surface area and porosimetry (ASAP) and Fourier transform infrared spectroscopy (FT-IR). The performance on nickel ions adsorption was assessed, in detail, in terms of adsorption kinetics and isotherm. The adsorption mechanism of nickel ions on ZIF-8 crystals was analyzed by Fourier transform infrared spectroscopy (FT-IR), and EDXS (energy-dispersive X-ray spectroscopy). The results can provide new insights to the application of ZIFs for water treatment.

2. Experimental

2.1. Materials

Zinc nitrate hexahydrate (Zn, $Zn(NO_3)_2 6H_2O$), 2-methylimidazole (Hmim, $C_4H_6N_2$) and EDTA were purchased from Merck commercially available chemicals. They were used without further purification. A stock solution of 1000 mg/L of nickel was prepared by dissolving necessary amount of nickel nitrate [$(Ni(NO_3)_2 \cdot 6H_2O)$] salt in Ultrapure water, acidified with nitric acid to prevent hydrolysis. All the solutions were made with ultrapure water. All volumetric flasks and vessels were cleaned by soaking in 10% HNO_3 for at least 24 h and rinsed several times with deionized (DI) water.

2.2. Synthesis of ZIF-8 crystals

ZIF-8 crystals were synthesized according to the route reported by Lestari [16]. Briefly, in a typical procedure, 0.29 g of Zn (2.5 mmol) was dissolved in 10 mL of DI water and then, was added to a solution consisting of 4.54 g of Hmim (0.15 mol) in 70 mL of DI water. After 5 min, it was transferred into a 100 ml Teflon autoclave and was heated in Memeret oven (Germany) at 120°C for 24 h. After cooling, the products were collected by repeated centrifugation (12000 rpm, 30 min), washed by DI water and methanol for four times, and finally were dried at 65°C overnight in a drying oven. The final molar composition of the synthesis solution was Zn^{2+}: Hmim: water = 1:70: 1200.

2.3. Batch nickel ions adsorption experiments

The nickel adsorption isotherms of ZIF-8 crystals were studied at pH 2–7. All the nickel adsorption experiments were carried out at environmental temperature (25°C). Before adsorption experiments, the ZIF-8 suspension was treated in an ultrasound bath for 5 min to avoid the aggregation of ZIF-8 crystals. Adsorption isotherm experiments were conducted in 250 mL shaking flasks containing 50 mL of nickel ions solution. The initial concentrations of nickel in the solution were 5, 20, 50 and 80 mg/L. The pH values of the solutions were adjusted to 2, 4, 6 and 7, using solutions of 0.01 mol/L HNO_3 and NaOH. After adding various amounts of ZIF-8 crystals (0.0125, 0.25, 0.5, 0.75 g/1000 ml) to the nickel ions solution, these flasks were shacked on a shaker for 24 h at 170 rpm. The equilibrium time (420 min) was determined from kinetic data when pH = 7, adsorbent dosage = 0.5

g/1000 ml, and initial nickel ions concentration = 20 mg/L. In each adsorption experiment, 50 mL of nickel ions solution of known concentration and pH was added to 0.5 g of ZIF-8 crystals in a 250 mL Erlenmeyer flask and the mixture was mixed by a rotary mixer (Heidolph, D-8420 Kelheim, Germany) at 170 rpm for 9 h. Then, the aqueous samples were centrifuged (Sigma 3-18KS) at 10000 rpm for 10 min to remove adsorbent and then they were analyzed for nickel ions.

The residual nickel ions in the solution were measured by an atomic absorption spectrometer. In order to obtain the adsorption capacity q_e, the amount of ions adsorbed per unit mass of adsorbent (mg/g) at equilibrium was calculated by using the following Eq. (1) [28].

$$q_e = \left(C_0 - C_e\right)\frac{v}{w} \tag{1}$$

where C_o and C_e (mg/l) are initial and equilibrium concentrations, respectively, V (L) is the volume of solution, and W (g) is the mass of the adsorbent.

Finally, C_o ions removal efficiency was calculated using Eq. (2) [29]:

$$\text{Removal efficiency } \% = \frac{\left(C_0 - C_e\right)}{C_e} \times 100 \tag{2}$$

2.4. Determination of pH point of zero charge (pH_{PZC})

The pH point of zero surface charge of ZIF-8 was determined using the solid addition method [30]. 50 ml of 0.01 M NaCl solution were transferred to a series of 250 ml stoppered conical flasks. The Initial pH (pH_i) values of the solutions were adjusted between 2 and 12 by adding either 0.1 M HCl or NaOH and were measured using a pH meter (Crison Basic 20). The pH_i of the solution was then accurately noted. 0.05 g of ZIF-8 was added to into the flask containing 50 ml of NaCl solution. The suspensions were kept shaking for 24 h in an air tight condition at 200 rpm and 25°C. The final pH values of the supernatant liquids were measured and noted. The difference between the initial and final pH (pH_f) values (ΔpH) was plotted vs. pH_i (x axis).The point of intersection of the resulting curve with the pH_i axis, i.e. at ΔpH = 0, gave the pH_{PZC}.

2.5. Desorption studies

Desorption of nickel ions from the spent ZIF-8 crystals was done with different concentrations of EDTA solution (0.05–0.1 M) and H_2O. The spent ZIF-8 crystals (0.5 g) were placed in a beaker with 100 mL of EDTA solution in the appropriate concentration and with 100 mL of H_2O. The solution pH was adjusted to 7.0 and the system was then mixed using a magnetic stirrer (Ika Werke GmbH, Germany) for the optimum contact time at T = 25°C; at the end of which the suspension was centrifuged and the concentrations of the desorbed nickel ions solutions were determined. All measurements of adsorption as well as desorption test were repeated three times. The presented values are averaged. The regenerated ZIF-8 sample was reused in three cycles after desorption of nickel using 0.1 M EDTA solution in experimental condition similar to first experiment.

2.6. Characterization

Powder XRD patterns were recorded at room-temperature on powder X-ray Diffractometer (Seifert, Germany 3003 PTS) with CuKa radiation (40 kV, 30 mA). The X-ray scanning speed was at a step size of 0.05° and 2 s step time from 5° to 50°. The relative crystallinities were calculated based on the six characteristic peaks of ZIF-8 at Bragg angles of 7.44, 10.48, 12.90, 14.87, 16.63 and 18.24 [14,31]. The surface morphologies and elemental compositions of products were examined by SEM (MIRA\\TESCAN) coupled with Energy-Dispersive X-ray Spectroscopy (EDX). The relative contents of nickel ions in sample were measured through EDX spectra. The pH of solution was measured by a pH meter (CRISON BASIC 20). FTIR spectra were taken on powder samples supported in KBr pellets with NEXUS 870 spectrometer in dry air at room temperature. Spectra were taken in the range of 500–4000 cm^{-1} in transmission mode. Nitrogen adsorption–desorption isotherms were measured at liquid nitrogen temperature (77 K) using a volumetric adsorption analyzer (Micromertics ASAP 2020). Before the porosity analysis, samples were pre-dried in an oven and then degassed for 6 h at 200°C. Brunauer-Emmett-Teller (BET) surface area, Langmuir model surface area, and micropore volume were calculated from the nitrogen adsorption–desorption isotherms. The total pore volume and micropore volume were calculated from the amount of nitrogen adsorbed at $P/P_\circ$ of 0.99 and via the t-plot method, respectively. The Barrett–Joyner–Halenda (BJH) method was applied to determine Pore-size distributions. Nickel ions concentration was measured by atomic absorption spectrometer machine (Shimadzu AA-670).

3. Results and discussion

3.1. Characterization of ZIF-8 crystals

Fig. 1a, presents XRD patterns of the ZIF-8 crystals. It can be seen that the synthesized ZIF-8 is highly crystal and the XRD patterns are in good agreement with previous observations [16]. Clearly, adsorption of nickel metal ions by ZIF-8 crystals has no obvious effect on the crystallinity of ZIF-8, while the intensities of the X-ray peaks of ZIF-8 crystals are slightly lower than those of virgin ZIF-8 crystals. The observed decrease in peaks may be resulted from the absorption of nickel ions on the surface of ZIF-8 crystals. Morphology and chemical composition of the ZIF-8 samples were characterized by SEM (Fig. 1b, c) and EDX. The crystals of ZIF-8 sample are homogeneous with a hexagonal shape and the average particle size about 100–150 nm. Fig. 1c shows that there is no change in the morphology and particle size of ZIF-8 after adsorption process. The EDX spectra of the ZIF-8 sample (Fig. 1f) display the homogeneous distribution of C, N, and Zn elements in ZIF-8 nanoparticles. The percentage of Zn, N and C elements were of 31.84 wt%, 21.97 wt% and 46.20 wt%, respectively. Fig. 1g confirms the presence of nickel in the ZIF-8 sample after adsorption. N_2 adsorption-desorption isotherms of the ZIF-8 sample were investigated to analyze

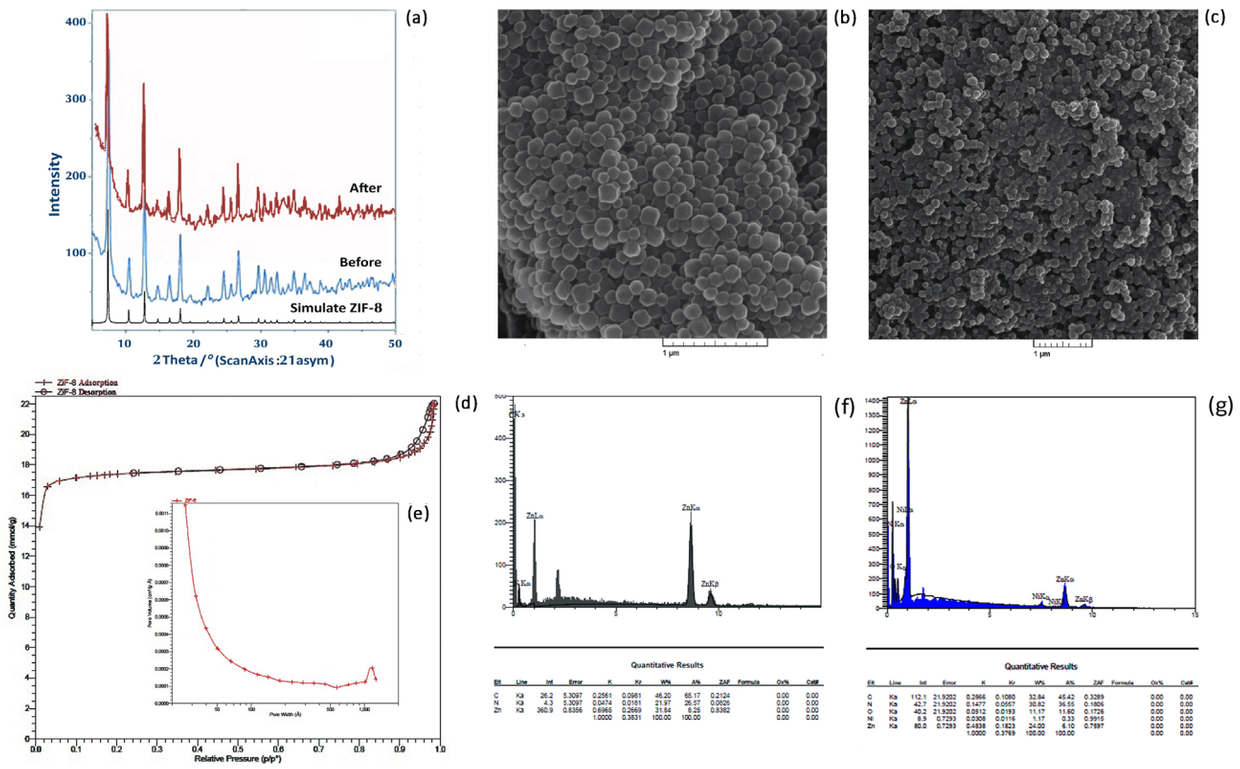

Fig.1. XRD diffraction patterns of (a) the simulated ZIF-8, synthesized ZIF-8 crystals and used ZIF-8 crystals after nickel adsorption, (b) FESEM images of ZIF-8 crystals before adsorption, (c) after nickel adsorption, (d) N_2 adsorption/desorption isotherms of ZIF-8 crystals, (e) Pore size distribution calculated from the desorption isotherm using the Barrett–Joyner–Halenda (BJH) method, (f) EDX spectra of ZIF-8 crystals sample before adsorption, (g) after adsorption.

the pore structure and specific surface area. As shown in Fig. 1d ZIF-8 exhibit typical type-I adsorption isotherm with high N_2 adsorption quantities at low pressure due to the micropores structures; while a second uptake at high relative pressure indicates the existence of textural mesoporosity formed by packing of ZIF-8 crystals. Total pore volume and micropores volume of the resulting ZIF-8 are about 0.73 and 0.55 cm^3/g, respectively. BET and Langmuir surface areas are 1303 and 1716 m^2/g, respectively and These values are relatively close to the ones reported in the literature [16]. Pore size distribution of the prepared ZIF-8 calculated from the desorption isotherm using the Barrett–Joyner–Halenda (BJH) method (Fig. 1e) indicates the presence of micropores with an average pore diameter less than 5 nm. The step originates from interparticle mesopores, proving the both micro and mesoporosity of the ZIF-8 crystals powders. There are some beneficial effects of mesoporosity of the adsorbents for fast mass transport kinetics; the existence of mesopores can also help to easily regeneration of the used adsorbents [32,33]. Figs. 2a, b show the adsorbent's FTIR spectra, before and after adsorption of nickel ions, respectively. The changes in the surface functional groups of of ZIF-8 after adsorption of nickel ions were also confirmed by FTIR spectra through the changes in the positions of some the peaks as well as the appearance of some new peaks. The band at 2956 cm^{-1} is attributed to the C-H stretching mode of the methyl group while the peak at 3135 cm^{-1} is attributed to the aromatic C–H stretch of the imidazole; the band in the range of about 3250–3400 cm^{-1} is due to the N-H bond stretch. The peak at 1584 cm^{-1} can be assigned to the C=N stretch in the imidazole ring [34]. The peak at 1678 cm^{-1} is attributed to the bending N–H vibration of the Hmim [35]. The intense and convoluted bands at 1427 cm^{-1} are associated with the entire ring stretching. The bands at 690 and 755 cm^{-1} in the finger print region are associated with out-of-plane bending of the Hmim ring (675–900 cm^{-1}), whereas peaks in the region of between 900 and 1350 cm^{-1} arise from the in-plane bending [36]. A peak at 1308 cm^{-1} can be assigned to the C-N-C stretch mode. There is a FT-IR band at 3629 cm^{-1} and a broad absorption band at around 3420 cm^{-1} for the as-prepared ZIF-8. These two bands are assigned to free hydroxyl groups and hydrogen bonded hydroxyl groups, respectively [37]. Due to the limitation of our IR apparatus (i.e., for mid-IR measurements only), the most interesting Zn–N stretch mode which is expected at 421 cm^{-1} cannot be observed. The FTIR spectrum of ZIF-8 crystals indicates significant changes after adsorption. The shifts in peak frequencies of C-H, N-H and O-H indicate that there are binding processes taking place on the surface of ZIF-8 crystals. Meantime, the bond at 531.76 cm^{-1} is disappeared, as it is shown in Fig. 2b, the 531.76 cm^{-1} peak corresponds to nickel oxides exchange which have taken place from 531 to 821 cm^{-1}. Further difference between Fig. 2a and Fig. 2b illustrated in new peak

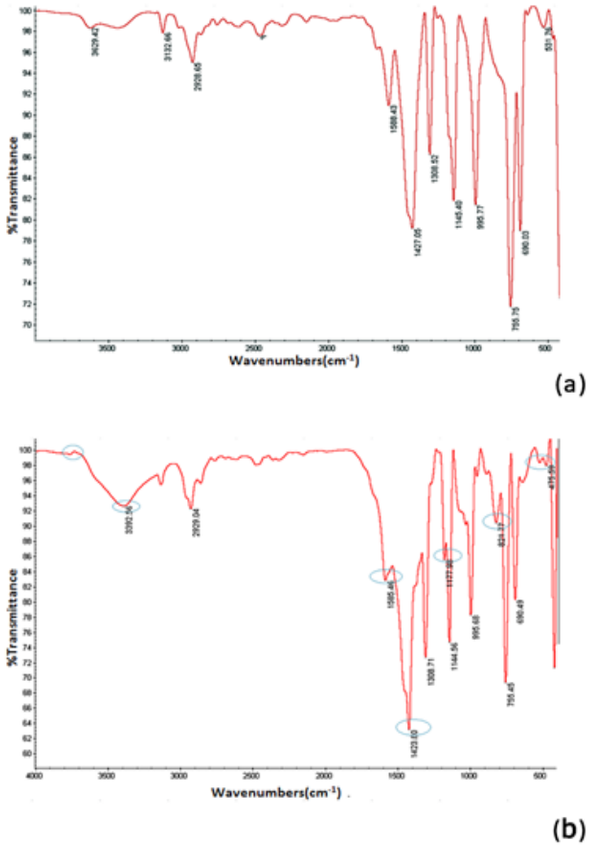

Fig. 2. FT-IR spectra of ZIF-8 crystals before (a) and after (b) nickel ions adsorption.

is detected at 1177 cm^{-1} (a short shoulder beside later 1144 cm^{-1} peak) could be as pi to nickel interactions.

3.2. pH point of the adsorbent zero charge

The point of zero charge (pH_{PZC}) of an adsorbent is the pH value at which the total number of positive and negative charges on its surface becomes zero. The pH at the point of adsorbent zero charge (pH_{PZC}) was measured by using the pH drift method [38]. It can be seen from Fig 3 that the surface charge of the ZIF-8 adsorbent is equal to 9.2, where the ΔpH values are zero [39]. After nickel ions loading, the pH_{PZC} of ZIF-8 crystals decreased from 9.2 to about 6.1. These results indicate that inner-sphere surface complexes may be occurred during the nickel ions adsorption process on ZIF-8 crystals, because when outer-sphere surface complexes are formed, the nickel adsorption is strongly dependent on ionic strength and cannot shift the pH_{PZC} of ZIF-8 crystals [40,41].

3.3. Adsorption isotherms

In order to investigate the adsorption isotherm, Langmuir and Freundlich isotherm models were analyzed:

In the Langmuir model, metal ions occur on a homogenous surface by monolayer adsorption without any interaction between the adsorbed ions. The linear form of the Langmuir equation demonstrated as follows [42]:

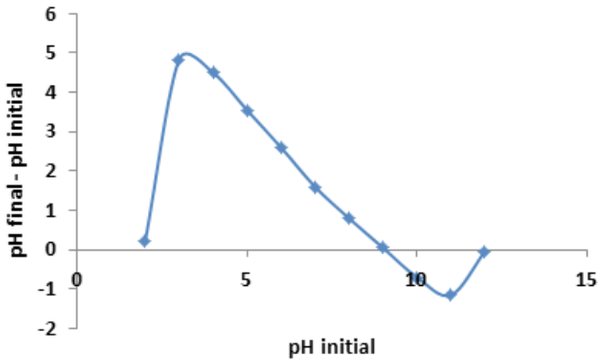

Fig. 3. pH point of zero charge (pHpzc) of the synthesized ZIF-8 crystals.

Table 1
Isotherm constants for adsorption of nickel ions onto the ZIF-8 crystals

Langmuir constants			Freundlich constants		
q_m (mg/g)	K_L (L/mg)	R^2	K_f	n	R^2
63.29	0.589	0.9961	20.89	5.2	0.8878

$$\frac{C_e}{q_e} = \frac{1}{q_m K_L} + \frac{C_e}{q_m} \tag{3}$$

where C_e is the equilibrium concentration of remaining nickel ions in the solution (mg/L), q_e is the amount of nickel ions adsorbed per mass unit of adsorbent at equilibrium (mg/ g), q_m is the monolayer adsorption capacity (mg/g), and b is the Langmuir constant (L/mg). The values of q_m and K_L can be determined from the linear plot of C_e/q_e vs. C_e. The linear plot of the Langmuir isotherm is shown in Fig. 4a, while the model parameters are listed in Table 1.

The Freundlich model assumes that the uptake of metal ions occur on a heterogeneous surface by monolayer adsorption. Linear expression of this model is given by the following equation [43]:

$$\log q_e = \log K_f + \frac{1}{n}\log C_e \tag{4}$$

where K_f and $1/n$ are the Freundlich constants characteristic of the system indicating the adsorption capacity and the adsorption intensity, respectively. Fig. 4b shows the applicability of this equation on the adsorption of nickel ions on ZIF-8 crystals. By plotting $\log q_e$ vs. $\log C_e$, values of K_f and n can be determined from the slope and intercept of the plot. When the Freundlich isotherm is applied to data obtained from Fig. 4b, the correlation coefficient (R^2) is approximately 0.887. However, the Langmuir correlation coefficients are found to be higher than 0.996. According to the results, the data fitted reasonably well on the Langmuir isotherm in the adsorption studies carried out by ZIF-8 crystals. Isotherm

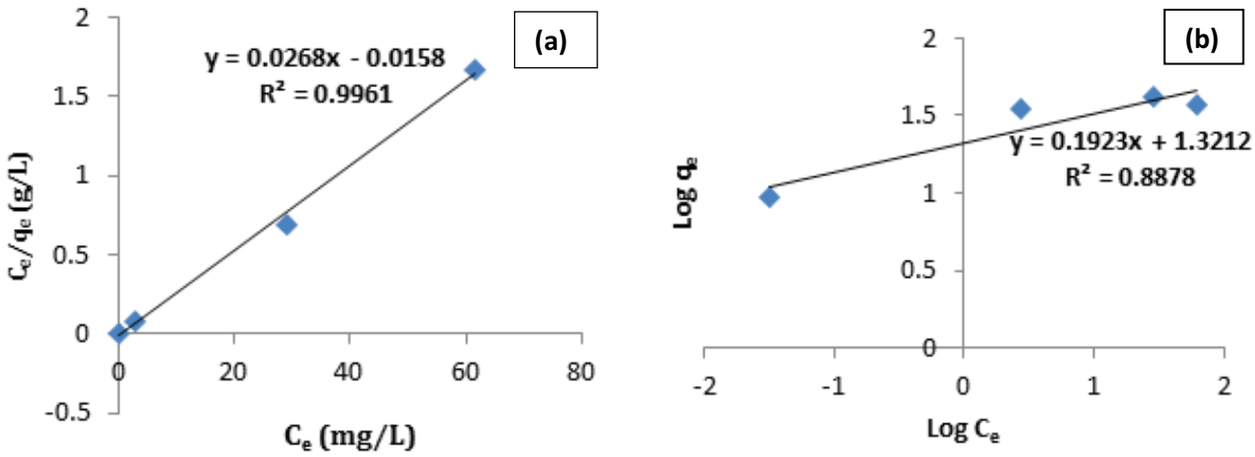

Fig. 4. Linear plots of Langmuir isotherm (a) and Freundlich isotherm (b) for nickel ions adsorption onto the ZIF-8 crystals.

constants for adsorption of nickel ions onto the ZIF-8 crystals are given in Table 1.

3.3. Adsorption kinetics

In order to evaluate the kinetic mechanism that controls the adsorption process, the three most widely used kinetic models, i.e. pseudo-first-order [44], pseudo-second-order [45] linear forms and intra-particle diffusion [46] were used. The pseudo-first-order equation is generally represented as follows:

$$\log\left(q_e - q_t\right) = \log q_e - \frac{K_1}{2.303}t \tag{5}$$

The first-order rate constants k_1 and q_e can be determined from the slopes and intercept of plots of log $(q_e - q_t)$ vs. t as shown in Fig.5.

The pseudo-second–order kinetic model has been linearized into four different types which are shown in Table 2 [47–49]. The most popular linear form is Type 1 equation. Figs. 6a–d show experimental data with linear equations of the four pseudo-second–order kinetic models obtained using the linear method for the adsorption of the under investigated nickel ions onto ZIF-8 crystals. Values of the first and second-order kinetic model constants, k_1 (min^{-1}) and k (mg/g·min), the amount of the nickel ions (mg/g) adsorbed at equilibrium, q_e, and the amount of the nickel ions (mg/g) adsorbed at time t, q_t, are listed in Table 3. In the case of the pseudo-second-order kinetics model of type 2, the regression (R^2) values calculated from the slopes of the curves shown in Fig. 6b, was 0.976 that there was a good agreement between the kinetic data of adsorption with the pseudo-second-order kinetics model of type 2.

The mechanism of nickel ions adsorption from aqueous solutions by ZIF-8 crystals was investigated using the intra-particle diffusion model. Since the pseudo first-order and the pseudo-second-order kinetic models provide little information about diffusion mechanism, the kinetic results were then analyzed by using the intra-particle diffusion model to determine the diffusion mechanism.

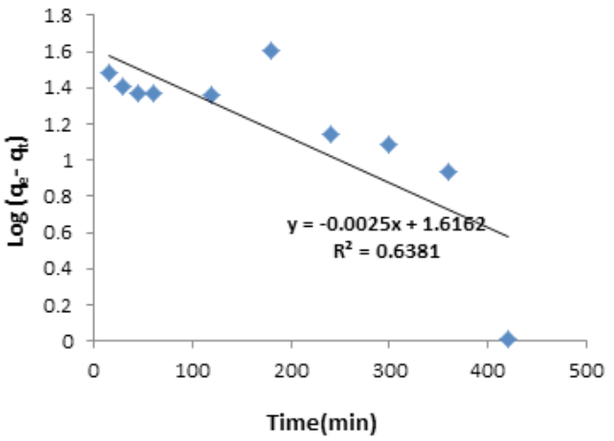

Fig. 5. Pseudo-first-linear equation obtained by using the linear equations obtained from the linear method for the sorption of nickel ions onto the ZIF-8 crystals.

Table 2
Pseudo-second order kinetic model linear forms

Type	Linear form	Plot	Parameter
Type 1	$\frac{t}{q_t} = \frac{1}{(Kq_e^2)} + \frac{1}{q_e}t$	t/q_t vs t	q_e = 1/slope
Type 2	$\frac{1}{q_t} = \left(\frac{1}{Kq_e^2}\right)\frac{1}{t} + \frac{1}{q_e}$	$1/q_t$ vs $1/t$	q_e =1/intercept K = intercept
Type 3	$q_t = q_{e-\left(\frac{1}{Kq_e^2}\right)\frac{q_t}{t}}$	q_t vs q_t/t	q_e = intercept K = –1/intercept x slope
Type 4	$\frac{q_t}{t} = Kq_e^2 - kq_e^2q_t$	q_t/t vs q_t	q_e = -intercept/slope K = slope^2/intercept

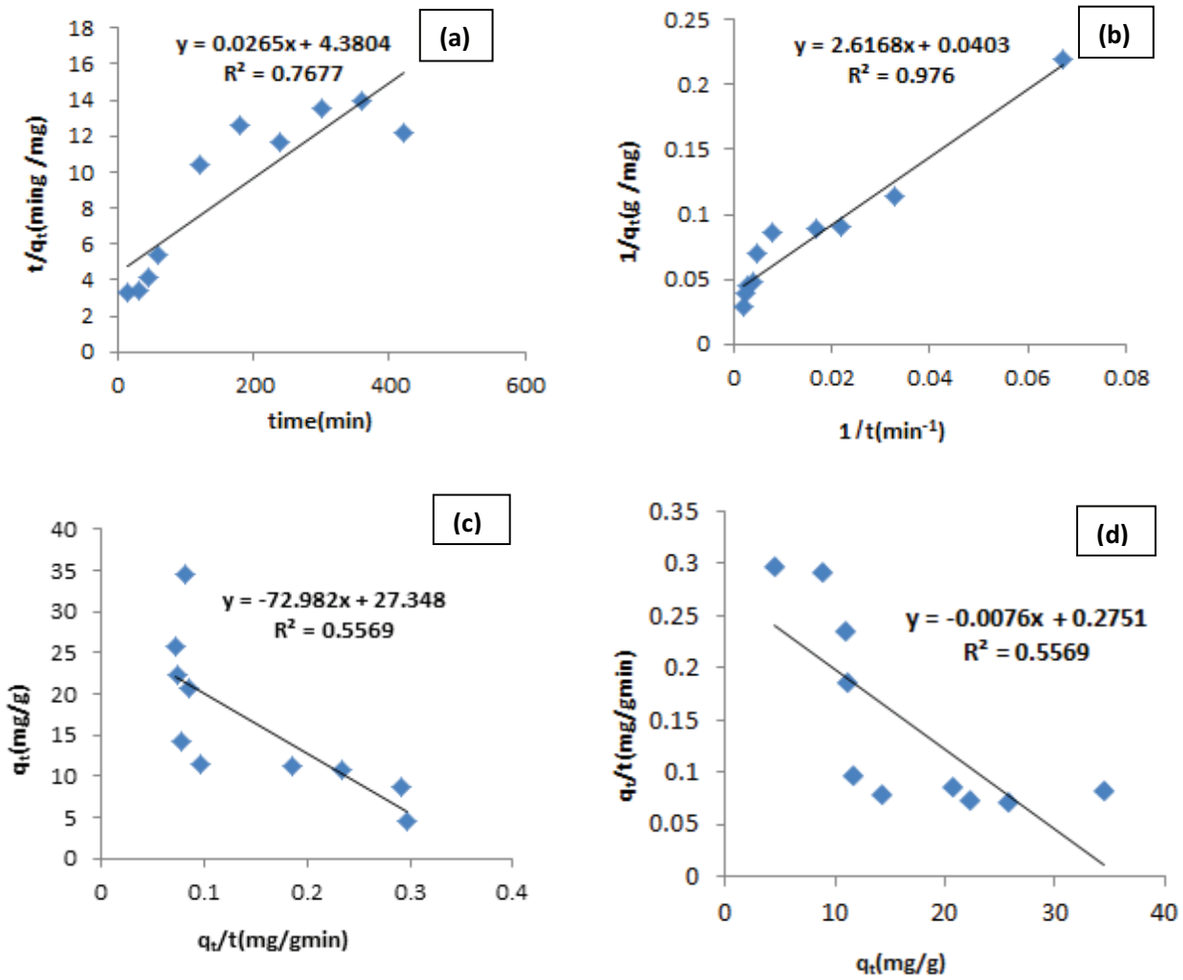

Fig.6. Type 1 pseudo-second-linear equation, (a) Type 2 pseudo-second-linear equation, (b). Type 3 pseudo-second-linear equation, (c) and Type 4 pseudo-second-linear equation, (d). obtained by using the linear equations obtained from the linear method for the sorption of nickel ions onto the ZIF-8 crystals.

The intraparticle diffusion equation is the following:

$$Q_t = K_d t^{1/2} + C \quad (6)$$

A linear plot of Q_t vs. $t^{1/2}$ representing the intra-particle diffusion model. The values of k_d and C can be calculated from the slope and intercept, respectively (Table 3). According to the equation for intra particle diffusion mechanism, the plot of Q_t vs. $t^{1/2}$ should be linear if intra-particle diffusion is the only mechanism applicable. Fig. 7 shows that for nickel ions, the plots are not linear and do not pass through the origin implying that intra particle diffusion mechanism is not the only mechanism involved in the sorption of nickel ions. It can be deduced therefore that the sorption of nickel ions by ZIF-8 crystals involve both physisorption and chemisorption processes.

3.4. Comparison of ZIF-8 crystals with other adsorbents

The values of maximum adsorption capacities of ZIF-8 adsorbent for the removal of nickel ions are compared with

Table 3
Kinetics constants obtained by using the linear methods for the adsorption of nickel

Pseudo-second-order models			
	k (L/min)	q_e (mg/g)	R^2
Type 1	0.0001	37.7	0.767
Type 2	0.0006	24.81	0.976
Type 3	0.0005	27.35	0.556
Type 4	0.0002.	36.2	0.556
Pseudo-first-order model			
K_1 (mg/g·min)	q_e (mg/g)	R^2	
0.0057	41.32	0.638	
Intra-particle diffusion model			
K_d	C	R^2	
1.45	1.15	0.899	

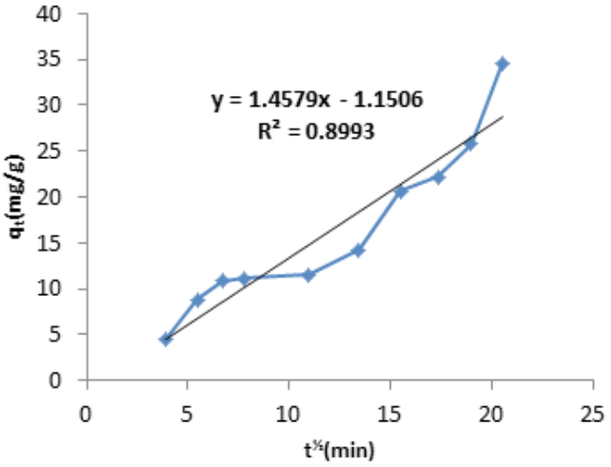

Fig. 7. Intraparticle diffusion mechanism for the adsorption of nickel ions onto ZIF-8 crystals.

Table 4
Maximum capacity, q_m (mg/g) for adsorption of nickel ions by various adsorbents

Adsorbent	q_m (mg/g)	Reference
Parthenium hysterophorus	17.24	[50]
Rice husk	44.6	[51]
Multiwalled carbon nanotubes	6.09	[52]
Peat	61.27	[53]
Waste silica modified iron oxide	2.61	[54]
Delonix regia pods	9.98	[55]
Natural coated sand	1.08	[56]
Watermelon rind	35.30	[57]
wMNR	15.15	[58]
Waste of tea factory	15.26	[59]
Treated algae	44.2	[60]
ZIF-8 crystals	69.4	This study

those of other adsorbents as shown in Table 4. The results in Table 4 indicate that ZIF-8 crystals have comparable adsorption capacities with other adsorbents.

3.5. Effect of contact time and initial metal ion concentration

Fig. 8. shows the results for the effect of contact time on the amount of nickel ions removed from aqueous solution at an initial concentration of 20 (mg/L). The obtained results show that the adsorption increases by increasing contact time. It is clear from the graph that the rate of nickel ions sorption is slow, attaining equilibrium in 420 min. The relationship between the initial nickel ions concentration of the solution and the amount of nickel ions removed from aqueous solution is shown in Fig. 9. The figure indicates that when the concentration of nickel ions became higher, the amount of nickel ions removed from aqueous solution decreased since the numbers of available sites for adsorption are reduced due to saturation of adsorption sites. At a

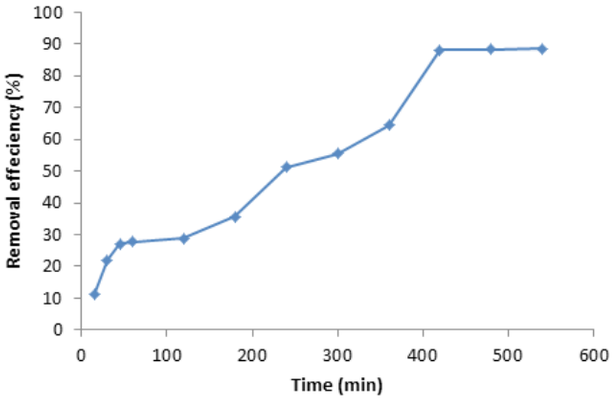

Fig. 8. Effect of contact time on nickel ions removal by ZIF-8 crystals; (pH = 7, adsorbent dose = 0.5 g/1000 ml rotating speed = 170 rpm).

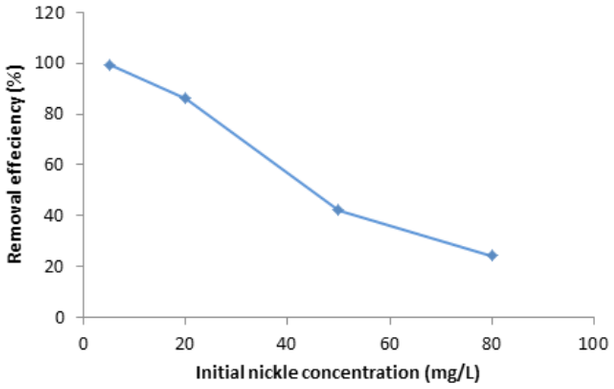

Fig. 9. Effect of initial nickel concentration on nickel ions removal by ZIF- crystals; (pH = 7, adsorbent dose = 0.5 g/1000 ml, rotating speed = 170 rpm and contact time = 24 h).

higher concentration of nickel ions, the ratio of initial number of moles of nickel ions to the adsorption sites available was higher, resulting in lower adsorption percentage, but the uptake of nickel ions increases with the increment of initial nickel ions concentration from 5 to 80 mg/l. At lower metal ions concentrations, the uptake is higher due to the larger surface area of the adsorbent being available for adsorption [61]. Moreover, with increasing the nickel ions concentration in the solution, the diffusion of nickel ions in the boundary layer increases resulting in higher sorption by ZIF-8 crystals.

3.6. Effect of pH

The effect of pH on the adsorption of nickel ions by ZIF-8 crystals in the range of 2–7. The pH of the aqueous solution is an important parameter that controls the adsorption process. Adsorption of different metals can be optimized at different pH values [62]. Moreover, the sorption of nickel ions by ZIF-8 crystals is also influenced by the surface properties of the sorbent and nickel ions presented in aqueous solution. However, the determination of the pH

point of zero charge (pH_{PZC}) can well explain and optimize nickel uptake on adsorbents at different pH ranges. It can be seen that pH_{PZC} of the ZIF-8 crystals is around 9.2; the value of pH_{PZC} implies that the surface of the ZIF-8 crystals is positively charged when solution pH is below 9.6, while the surface of ZIF-8 crystals becomes negatively charged at solution pH above 9.2. Fig. 10. shows the nickel adsorption on ZIF-8 at different solution pH. It can be observed that there is an increase in uptake of nickel ions from 0.8 to 69.4 mg/g in solution with increased pH from 2 to 7 [63]. At low pH values, H^+ ions compete with nickel ions for the surface of the adsorbent which would hinder the nickel ions from reaching the binding sites of the adsorbent caused by repulsive forces. Also, the lower removal of nickel ions at pH 2–5 may be attributed to the solubility of used ZIF-8 nano adsorbent. ZIF-8 is unstable under acidic pH conditions and high concentration of Zn^{2+} was released into the solution indicating the dissolution of ZIF-8 crystals [36]. A higher pH value (7) can lead to more precipitation of metal hydroxides due to increase in hydroxide anion.

3.7. Effect of adsorbent dose

The effect of varying amounts of ZIF-8 crystals in the range of 0.0125–0.75 g/L on the adsorption of nickel ions (20 mg/L) from aqueous solutions was shown in Fig. 11. The pH was adjusted to 7.0 using 1 M HNO_3 or 1 M NaOH. The data show that the adsorption increases as the amount of ZIF-8 crystals increases which may be attributed to an increase in the number of binding sites available to adsorb metal ions. Moreover, 0.5 g/L dose of ZIF-8 crystals was an optimum one for further experiments.

3.8. Desorption test

The regeneration of the ZIF-8 crystals after adsorption is critical for its economic viability in practical applications. For this purpose a desorption test was carried out, using H_2O and EDTA solution in various concentrations (0.05 and 0.1 M) as the regenerating agent. The results presented in Table 5 indicate that H_2O is a weak desorbing agent. This is evidence of a strong bond between the adsorbate and adsorbent. Only when EDTA solution was used a significant increase in the degree of desorption achieved. Higher desorption efficiency was found to be obtainable if the concentration of the EDTA solution used as a desorbing agent increased. After regeneration, the sorbent was used again in four successive cycles. No significant difference in nickel adsorption capacity of ZIF-8 crystals was observed after two consecutive cycles. During regeneration, 93% of the removed arsenic was recovered in the first cycle, and then, 87–83.3% arsenic was recovered in the subsequent cycles, but the recovery of nickel ions was reduced to 50.6 on fourth cycle (Fig. 12). The decrease in the adsorption capacity after

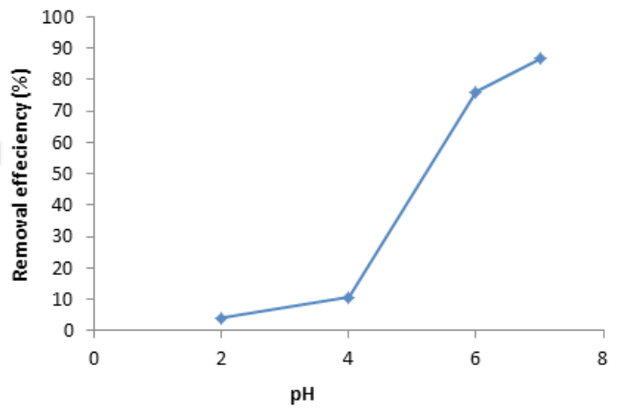

Fig. 10. Effect of pH on the removal of nickel ions by ZIF-8 crystals; (initial nickel concentration = 20 mg/L, adsorbent dose = 0.5 g/1000 ml, rotating speed = 170 rpm and contact time = 24 h).

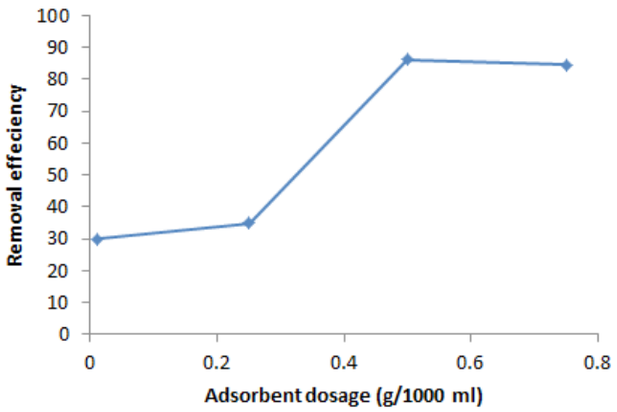

Fig. 11. Effect of adsorbent dose on nickel removal by ZIF-8 crystals; (pH = 7, initial nickel concentrations = 5, 20, 50, 80 mg/L, rotating speed = 170 rpm and contact time = 24 h).

Table 5
Desorption of nickel ions from the spent ZIF-8 crystals using H_2O and EDTA solution

Initial metal ion concentration (mg/L)	Desorption percentage (%)		
	H_2O	EDTA 0.05 M	EDTA 0.1 M
20	45	75	93

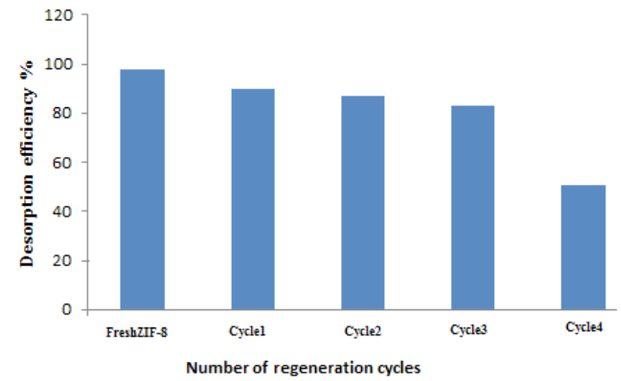

Fig. 12. The regeneration cycles of ZIF-8 for the adsorption of nickel at pH 7.0.

four repeated cycles may be due to the accumulation of the un-desorbed nickel ions on some active sites of ZIF-8 nanoadsorbant resulting in partial blockage of the active sites. In addition, the capacity reduction may also be due to loss of some ligand moieties from the surface of ZIF-8 after a few desorption cycles [64].

4. Conclusion

In summary, the ZIF-8 crystals were prepared by hydrothermal synthesis. The morphology of ZIF-8 crystals by scanning electron microscope (SEM) shows nanoparticle formation with a high surface area of 1303 m^2/g. Fourier transform infrared spectroscopy (FT-IR) reveals the functional groups of ZIF-8 crystals and the interaction with nickel ions, the hydroxyl and amine groups of crystals provide adsorption sites for nickel ions. ZIF-8 crystals possess high crystallinity by XRD pattern. The experiments were shown that ZIF-8 crystals are an effective adsorbent for the removal of nickel ions from aqueous solutions. The adsorption process was a function of the adsorbent dosage, initial nickel ions concentration, pH and time. Isotherm studies indicated that the Langmuir model fitted the experimental data better than Freundlich model. The adsorption equilibrium was described well by the Langmuir isotherm model with maximum adsorption capacity of 69.36 mg/g of nickel ions on ZIF-8 crystals. The kinetic behavior of metal toward the ZIF-8 crystals was well fitted by pseudo-second-order order Kinetics model of type 2 with regression value of 0.976 and the result also indicated the presence of intraparticle diffusion on the sorption of nickel ions, although it was not the sole rate determining step. It can be deduced therefore that the sorption of Nickel ions by ZIF-8 crystals involve both physisorption and chemisorption Processes. The result obtained from the desorption study show that 0.1 M EDTA solution to be suitable for desorption of nickel from the spent ZIF-8 crystals even after four adsorption/desorption cycles. No reduction in adsorption efficiency was observed up to 3 cycles of adsorption–desorption studies.

References

[1] A.K. Meena, K. Kadirvelu, G.K. Mishra, C. Rajagopal, P.N. Nagar, Adsorptive removal of heavy metals from aqueous solution by treated sawdust (Acacia arabica), J. Hazard. Mater., 150 (2008) 604–611.
[2] S. Mirbagheri, Optimization of motor vehicle industries wastewater treatment methods with the aim of heavy metals removal and water reuse in pilot scale, J. Environ. Health. Sci. Eng., 3 (2006) 289–295.
[3] P.M. Choksi, V.Y. Joshi, Adsorption kinetic study for the removal of nickel (II) and aluminum (III) from an aqueous solution by natural adsorbents, Desalination, 208 (2007) 216–231.
[4] N. Khellaf, M. Zerdaoui, Growth response of the duckweed Lemna minor to heavy metal pollution, J. Environ. Health. Sci. Eng., 6 (2009) 161–166.
[5] E. Malkoc, Ni (II) removal from aqueous solutions using cone biomass of Thuja orientalis, J. Hazard. Mater., 137 (2006) 899–908.
[6] A. Ewecharoen, P. Thiravetyan, E. Wendel, H. Bertagnolli, Nickel adsorption by sodium polyacrylate-grafted activated carbon, J. Hazard. Mater., 171 (2009) 335–339.
[7] A. Bhatnagar, A. Minocha, Biosorption optimization of nickel removal from water using Punica granatum peel waste, Colloids Surf., B., 76 (2010) 544–548.
[8] F. Ciesielczyk, P. Bartczak, K. Wieszczycka, K. Siwińska-Stefańska, M. Nowacka, T. Jesionowski, Adsorption of Ni (II) from model solutions using co-precipitated inorganic oxides, Adsorpt., 19 (2013) 423–434.
[9] P. Rudnicki, Z. Hubicki, D. Kołodyńska, Evaluation of heavy metal ions removal from acidic waste water streams, Chem. Eng. J., 252 (2014) 362–373.
[10] Ł. Klapiszewski, P. Bartczak, M. Wysokowski, M. Jankowska, K. Kabat, T. Jesionowski, Silica conjugated with kraft lignin and its use as a novel 'green'sorbent for hazardous metal ions removal, Chem. Eng. J., 260 (2015) 684–693.
[11] E. Iakovleva, E. Mäkilä, J. Salonen, M. Sitarz, M. Sillanpää, Industrial products and wastes as adsorbents for sulphate and chloride removal from synthetic alkaline solution and mine process water, Chem. Eng. J., 259 (2015) 364–371.
[12] Z. Veličković, G.D. Vuković, A.D. Marinković, M.S. Moldovan, A.A. Perić-Grujić, P.S. Uskoković, M.D. Ristić, Adsorption of arsenate on iron (III) oxide coated ethylenediamine functionalized multiwall carbon nanotubes, Chem. Eng. J., 181 (2012) 174–181.
[13] A. Phan, C.J. Doonan, F.J. Uribe-Romo, C.B. Knobler, M. O'keeffe, O.M. Yaghi, Synthesis, structure, and carbon dioxide capture properties of zeolitic imidazolate frameworks, Acc. Chem. Res., 43 (2010) 58–67.
[14] K.S. Park, Z. Ni, A.P. Côté, J.Y. Choi, R. Huang, F.J. Uribe-Romo, H.K. Chae, M. O'Keeffe, O.M. Yaghi, Exceptional chemical and thermal stability of zeolitic imidazolate frameworks, Proceedings of the National Academy of Sciences., 103 (2006) 10186–10191.
[15] R. Banerjee, A. Phan, B. Wang, C. Knobler, H. Furukawa, M. O'keeffe,, O.M. Yaghi, High-throughput synthesis of zeolitic imidazolate frameworks and application to CO_2 capture, Science., 319 (2008) 939–943.
[16] G. Lestari, Hydrothermal Synthesis of Zeolitic Imidazolate Frameworks-8 (ZIF-8) Crystals with Controllable Size and Morphology, PhD diss., 2012.
[17] D. Ge, H.K. Lee, Water stability of zeolite imidazolate framework 8 and application to porous membrane-protected micro-solid-phase extraction of polycyclic aromatic hydrocarbons from environmental water samples, J. Chromatogr. A., 1218 (2011) 8490–8495.
[18] C. Chizallet, S. Lazare, D. Bazer-Bachi, F. Bonnier, V. Lecocq, E. Soyer, A.A. Quoineaud, N. Bats, Catalysis of transesterification by a nonfunctionalized metal-organic framework: acido-basicity at the external surface of ZIF-8 probed by FTIR and ab initio calculations, J. Am. Chem. Soc., 132 (2010) 12365–12377.
[19] C. Gücüyener, J. van den Bergh, J. Gascon, F. Kapteijn, Ethane/ethene separation turned on its head: selective ethane adsorption on the metal-organic Framework ZIF-7 through a gate-opening mechanism, J. Am. Chem. Soc., 132 (2010) 17704–17706.
[20] Wu. H.W. Zhou T. Yildirim, Hydrogen storage in a prototypical zeolitic imidazolate framework-8, J. Am. Chem. Soc., 129 (2007) 5314–5315.
[21] O. Karagiaridi, M.B. Lalonde, W. Bury, A.A. Sarjeant, O.K. Farha, J.T. Hupp, Opening ZIF-8: a catalytically active zeolitic imidazolate framework of sodalite topology with unsubstituted linkers, J. Am. Chem. Soc., 134 (2012) 18790–18796.
[22] M.R. Samarghandi, S. Azizian, M.S. Siboni, S.J. Jafari, S. Rahimi, Removal of divalent nickel from aqueous solutions by adsorption onto modified holly sawdust: equilibrium and kinetics, Iran. J. Environ. Health. Sci. Eng., 8 (2011) 181.
[23] K. Kadirvel, K. Thamaraiselvi, C. Namasivayam, Adsorption of nickel (II) from aqueous solution onto activated carbon prepared from coirpith, Sep. Purif. Technol., 24 (2001) 497–505.
[24] M. Ghasemi, N. Ghasemi, G. Zahedi, S.R.W. Alwi, M. Goodarzi H. Javadian, Kinetic and equilibrium study of Ni(II) sorption from aqueous solutions onto Peganum harmala-L, Int. J. Environ. Sci. Technol., 11 (2014) 1835–1844.

[25] H. Hasar, Adsorption of nickel(II) from aqueous solution onto activated carbon prepared from almond husk, J. Hazard. Mater., 97 (2003) 49–57.
[26] S.Y. Kocaoba, Orhan, T. Akyüz, Kinetics and equilibrium studies of heavy metal ions removal by use of natural zeolite, Desalin., 214 (2007) 1–10.
[27] Lu. X.Y.-x. Hu, B.-h. Zhang, Kinetics and equilibrium adsorption of copper (II) and nickel (II) ions from aqueous solution using sawdust xanthate modified with ethanediamine, Trans. Nonferrous Met. Soc. China., 24 (2014) 868–875.
[28] S.N. do Carmo Ramos, A.L.P. Xavier, F.S. Teodoro, Elias, M.M.C. Gonçalves, F.J. Gil, L.F., de Freitas, R.P. Gurgel, L.V.A., Modeling mono-and multi-component adsorption of cobalt (II), copper (II), and nickel (II) metal ions from aqueous solution onto a new carboxylated sugarcane bagasse. Part I: Batch adsorption study, Ind. Crops Prod., 74 (2015) 357–371.
[29] F. Fang, L. Kong, J. Huang, S. Wu, K. Zhang, X. Wang, B. Sun, Z. Jin, J. Wang, X.J. Huang, J. Liu, Removal of cobalt ions from aqueous solution by an amination graphene oxide nanocomposite, J. Hazard. Mater., 270 (2014) 1–10.
[30] M.S. Onyango, Y. Kojima, O. Aoyi, E.C. Bernardo, H. Matsuda, Adsorption equilibrium modeling and solution chemistry dependence of fluoride removal from water by trivalent-cation-exchanged zeolite F-9, J. Colloid Interface Sci., 279 (2004) 341–350.
[31] N.K. Demir, B. Topuz, L. Yilmaz, H. Kalipcilar, Synthesis of ZIF-8 from recycled mother liquors, Microporous Mesoporous Mater., 198 (2014) 291–300.
[32] J. Cravillon, R. Nayuk, S. Springer, A. Feldhoff, K. Huber, M. Wiebcke, Controlling zeolitic imidazolate framework nano- and microcrystal formation: insight into crystal growth by time-resolved in situ static light scattering, Chem. Mater., 23 (2011) 2130–2141.
[33] B.K. Jung, J.W. Jun, Z. Hasan, S.H. Jhung, Adsorptive removal of p-arsanilic acid from water using mesoporous zeolitic imidazolate framework-8, Chem. Eng. J., 267 (2015) 9–15.
[34] M.J.C. Ordonez, K.J. Balkus, J.P. Ferraris, I.H. Musselman, Molecular sieving realized with ZIF-8/Matrimid® mixed-matrix membranes, J. Membr. Sci., 361 (2010) 28–37.
[35] Y. Shen, Y. Zhang, Q. Zhang, L. Niu, T. You, A. Ivaska, Immobilization of ionic liquid with polyelectrolyte as carrier, Chem. Commun., 33 (2005) 4193–4195.
[36] M. Jian, B. Liu, G. Zhang, R. Liu, X. Zhang, Adsorptive removal of arsenic from aqueous solution by zeolitic imidazolate framework-8 (ZIF-8) nanoparticles, Colloids Surf., A., 465 (2015) 67–76.
[37] S. Bratos, Profiles of hydrogen stretching ir bands of molecules with hydrogen bonds: a stochastic theory. I. Weak and medium strength hydrogen bonds, J. Chem. Phys., 63 (1975) 3499–3509.
[38] B.H. Hameed, Spent tea leaves: a new non-conventional and low-cost adsorbent for removal of basic dye from aqueous solutions, J. Hazard. Mater., 161 (2009) 753–759.
[39] J. Li, Y.N. Wu, Z. Li, B. Zhang, M. Zhu, X. Hu, Y. Zhang, F. Li, Zeolitic imidazolate framework-8 with high efficiency in trace arsenate adsorption and removal from water, J. Phys. Chem. C., 118 (2014) 27382–27387.
[40] Su, Y., H. Cui, Q. Li, S. Gao, J.K. Shang, Strong adsorption of phosphate by amorphous zirconium oxide nanoparticles, Water. Res., 47 (2013) 5018–5026.
[41] Z. Wang, S.W. Lee, J.G. Catalano, J.S. Lezama-Pacheco, J.R. Bargar, B.M. Tebo, D.E. Giammar, Adsorption of uranium (VI) to manganese oxides: X-ray absorption spectroscopy and surface complexation modeling, Environ. Sci. Technol., 47 (2012) 850–858.
[42] I. Langmuir, The constitution and fundamental properties of solids and liquids. 11. Liquids, J. Am. Chem. Soc., 3 (1917) 1848–1906.
[43] H. Freundlich, Over the adsorption in solution, J. Phys. Chem., 57 (1906) 470.
[44] S. Lagergren, About the theory of so-called adsorption of soluble substances, 4 (1898)1–39.
[45] Y. Ho, G. McKay, The kinetics of sorption of basic dyes from aqueous solution by sphagnum moss peat, Can. J. Chem. Eng., 76 (1998) 822–827.
[46] W.J. Weber, J.C. Morris, Kinetics of adsorption on carbon from solution, J. Sanitary. Eng. Div., 89 (1963) 31–60.
[47] D.G. Kinniburgh, C.J. Milne, M.F. Benedetti, J.P. Pinheiro, J. Filius, L.K. Koopal, W.H. Van Riemsdijk, Metal ion binding by humic acid: application of the NICA-Donnan model, Environ. Sci. Technol., 30 (1996) 1687–1698.
[48] E. Longhinotti, F. Pozza, L. Furlan, M.D.N.D.M. Sanchez, M. Klug, M. Laranjeira, V.T. Fávere, Adsorption of anionic dyes on the biopolymer chitin, J. Braz. Chem. Soc., 9 (1998) 435–440.
[49] Y.-S. Ho, Selection of optimum sorption isotherm, Carbon, 42 (2004) 2115–2116.
[50] H. Lata, V. Garg, R. Gupta, Sequestration of nickel from aqueous solution onto activated carbon prepared from Parthenium hysterophorus L, J. Hazard. Mater., 157 (2008) 503–509.
[51] R.M. Lattuada, M.C.R. Peralba, Dos Santos, J.H.Z., Fisch, A.G. Peat, rice husk and rice husk carbon as low-cost adsorbents for metals from acidic aqueous solutions, Sep. Sci. Technol., 49 (2014) 101–111.
[52] T. Abdel-Ghani, G.A. El-Chaghaby, F.S. Helal, Individual and competitive adsorption of phenol and nickel onto multiwalled carbon nanotubes, J. Adv. Res., 6 (2015) 405–415.
[53] P. Bartczak, M. Norman, Ł. Klapiszewski, N. Karwańska, M. Kawalec, M. Baczyńska, M. Wysokowski, J. Zdarta, F. Ciesielczyk, T. Jesionowski, Removal of nickel (II) and lead (II) ions from aqueous solution using peat as a low-cost adsorbent: A kinetic and equilibrium study, Arabian J. Chem., 2015.
[54] F. Unob, F. Unob, B. Wongsiri, N. Phaeon, M. Puanngam, J. Shiowatana, Reuse of waste silica as adsorbent for metal removal by iron oxide modification, J. Hazard. Mater., 142 (2007) 455–462.
[55] A.A. Festus, O.A. Elvis, A.B. Morayo, Equilibrium sorption of lead and nickel from solutions by flame of the forest (Delonix regia) pods: kinetics and isothermic study, J. Environ. Prot., 4 (2013) 261.
[56] N. Boujelben, J. Bouzid, Z. Elouear, Adsorption of nickel and copper onto natural iron oxide-coated sand from aqueous solutions: study in single and binary systems, J. Hazard. Mater., 163 (2009) 376–382.
[57] R. Lakshmipathy, N. Sarada, Application of watermelon rind as sorbent for removal of nickel and cobalt from aqueous solution, Int. J. Miner. Process., 122 (2013) 63–65.
[58] N.S. Randhawa, D. Dwivedi, S. Prajapati, R.K. Jana, Application of manganese nodules leaching residue for adsorption of nickel (II) ions from aqueous solution, Int. J. Environ. Sci. Technol., 12 (2015) 857–864.
[59] E. Malkoc, Y. Nuhoglu, Investigations of nickel (II) removal from aqueous solutions using tea factory waste, J. Hazard. Mater., 127 (2005) 120–128.
[60] V.K. Gupta, A. Rastogi, A. Nayak, Biosorption of nickel onto treated alga (Oedogonium hatei): application of isotherm and kinetic models, J. Colloid Interface Sci., 342 (2010) 533–539.
[61] P. SenthilKumar, S. Ramalingam, V. Sathyaselvabala, S.D. Kirupha, S. Sivanesan, Removal of copper (II) ions from aqueous solution by adsorption using cashew nut shell, Desalination, 266 (2011) 63–71.
[62] R. Wahi, D. Kanakaraju, N.A. Yusuf, Preliminary study on zinc removal from aqueous solution by sago wastes, Global J. Environ. Res., 4 (2010) 127–134.
[63] W.A. Carvalho, C. Vignado, J. Fontana, Ni (II) removal from aqueous effluents by silylated clays, J. Hazard. Mater., 153 (2008) 1240–1247.
[64] G. Ndayambaje, K. Laatikainen, M. Laatikainen, E. Beukes, O. Fatoba, N. van der Walt, L.L. Petrik, T. Sainio, Adsorption of nickel (II) on polyacrylonitrile nanofiber modified with 2-(2′-pyridyl) imidazole, Chem. Eng. J., 284 (2016) 1106–1116.